

# Effect of transverse and longitudinal magnetic field on the excess conductivity of $\text{YBa}_2\text{Cu}_{3-z}\text{Al}_z\text{O}_{7-\delta}$ single crystals with a given topology of plane defects

*R.V.Vovk, Z.F.Nazyrov, G.Ya.Khadzhai,  
V.M.Pinto Simoes<sup>\*, \*\*</sup>, V.V.Kruglyak<sup>\*\*\*</sup>*

V.Karazin Kharkiv National University, 4 Svoboda Sq., 61077 Kharkov, Ukraine  
\*Instituto Superior Dom Afonso III Convento Espirito Santo, 8100-641 Loule, Portugal

\*\*IPA\_Instituto Superior Autonomo de Estudos Politecnicos, Rua de Xabregas, 20, 1° 1900-440 Lisboa, Portugal

\*\*\*University of Exeter, Stocker road, Exeter, EX4 4QL, United Kingdom

*Received July 23, 2012*

The effect of a constant magnetic field to 12.7 kOe on the temperature dependences of electric conductivity of aluminum-doped  $\text{YBaCuO}$  single crystals with a system of unidirectional twinning boundaries has been investigated. It is determined that the twinning boundaries are effective centers of scattering of fluctuation carriers. Directly near  $T_c$  the temperature dependences of the excess paraconductivity are satisfactorily described by the Hikami-Larkin theoretical model of fluctuation conductivity for layered superconducting systems. The reasons for the suppression of three-dimensional superconducting fluctuations and the nonmonotonic dependence of  $\xi_c(0, H)$  in weak magnetic fields with the magnetic field vector oriented along  $c$  axis were discussed. It was shown that the lack of fan-shaped expansion of the resistive transitions in the magnetic field in these samples is conditioned by the lack of the no pinning vortex liquid phase due to increased pinning of the vortex lattice at the twin boundaries.

Исследовано влияние постоянного магнитного поля до 12,7 кЭ на температурные зависимости электропроводности в базовой  $ab$ -плоскости легированных алюминием монокристаллов  $\text{YBaCuO}$  с системой однонаправленных двойниковых границ. Установлено, что двойниковые границы являются эффективными центрами рассеяния флуктуационных носителей. Непосредственно вблизи  $T_c$  температурные зависимости избыточной парапроводимости удовлетворительно описываются в рамках теоретической модели флуктуационной проводимости Хиками-Ларкина для слоистых сверхпроводящих систем. Обсуждаются причины подавления трехмерных сверхпроводящих флуктуаций и немонотонной зависимости  $\xi_c(0, H)$  в слабых магнитных полях при ориентации вектора магнитного поля вдоль оси  $c$ . Показано, что отсутствие "веерообразного" расширения резистивных переходов в магнитном поле, характерного для беспримесных образцов  $\text{YBa}_2\text{Cu}_3\text{O}_{7-\delta}$ , обусловлено угнетением фазового перехода в состояние незапинингованной вихревой жидкости вследствие усиления пиннинга вихревой решетки на двойниковых границах.

## 1. Introduction

It is known that electro-transport properties of the anisotropic high-temperature su-

perconductor (HTSC) of  $\text{YBa}_2\text{Cu}_3\text{O}_{7-\delta}$  are strongly dependent upon the type and concentration of defects and oxygen

stoichiometry [1–3]. In YBCO, the small coherence length and the large penetration depth leads to the effective pinning of Abrikosov vortices, including the small-scale point defects [4]. Alloying YBCO with elements that substitute the copper atoms in CuO planes usually leads to a reduction of critical parameters and deterioration of electrical conductivity [1–3]. Alloying with aluminium leads to decrease of the critical temperature ( $T_c$ ) and of the secondary critical field ( $H_{c2}$ ) [1]. One of the characteristics of aluminium doped single crystals is the absence of the so-called "fan-shaped" expansion of the resistive transitions in magnetic field. Notably, this feature is always observed in pure  $\text{YBa}_2\text{Cu}_3\text{O}_{7-\delta}$  samples [4–7]. As a result there is a change of the fluctuation conductivity (FC), which is realized in these compounds at temperatures near but higher to the critical temperature ( $T > T_c$ ). It should also be noted that an additional source of anisotropy in  $\text{YBa}_2\text{Cu}_3\text{O}_{7-\delta}$  single crystals is the existence of twinning boundaries (TB) [8, 9], the influence of which on transport properties in the normal state has not been sufficiently studied, due to experimental difficulties in determining the contribution of these defects.

This anisotropy manifests itself in the form of a maximum critical current near the orientation of  $\mathbf{H} \parallel \text{TB}$  [6, 7], the reason of an appearance of which to date has not been established. Explanation of the mechanism of occurrence of this phenomenon is of interest both from the scientific and technological perspective.

On this basis in the present study we investigate electrical resistivity properties under constant magnetic fields up to 12.7 kOe with the orientation of the magnetic field  $\mathbf{H} \perp \mathbf{c}$  and  $\mathbf{H} \parallel \mathbf{c}$ , in the different conductivity types  $\text{YBa}_2\text{Cu}_{3-z}\text{Al}_z\text{O}_{7-\delta}$  of single crystals ( $z \leq 0.5$ ) with an unidirectional TB system and when the transport current is the following:  $\mathbf{I} \parallel \text{TB}$ , when the TB effect on the scattering processes is minimized.

## 2. Experimental

The single crystals  $\text{YBa}_2\text{Cu}_{3-z}\text{Al}_z\text{O}_{7-\delta}$  were grown in a gold crucible by the solution-melting method, under small temperature gradient along the crucible [2, 3]. This method allows us to select single crystals with dimensions  $5 \times 5 \text{ mm}^2$  in  $ab$ -plane and the third dimension between 0.02–0.05 mm. To obtain aluminium doped single crystals, we added

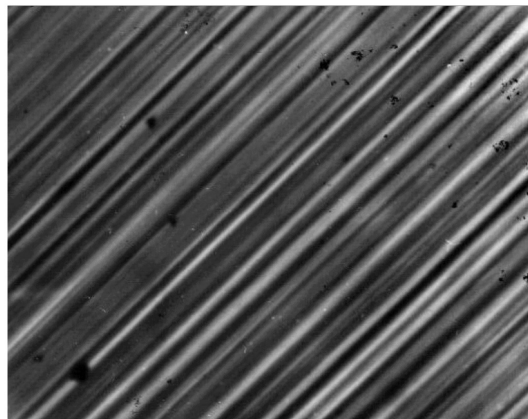


Fig. 1. Photograph of the singly-oriented TB areas of  $\text{YBa}_2\text{Cu}_{3-z}\text{Al}_z\text{O}_{7-\delta}$  single crystal, in polarized light ( $\times 440$ ).

0.2 wt. %  $\text{Al}_2\text{O}_3$ . As source components we used  $\text{Y}_2\text{O}_3$ ,  $\text{BaCO}_3$ ,  $\text{CuO}$ ,  $\text{Al}_2\text{O}_3$  powder compounds. To obtain oxygen saturating regime, the crystals were annealed in oxygen flow at the temperature of 430°C for three days. For the resistivity measurements the single crystals with unidirectional TBs with dimension of  $0.5 \times 0.5 \text{ mm}^2$  were selected (Fig. 1). This geometry was selected so that we could cut out bridges with parallel TB with a width of 0.2 mm at distances between the pair of contacts of 0.3 mm. The TBs within the bridges were oriented at one direction. The experimental geometry was selected so that the transport current vector in  $ab$ -plane  $\mathbf{I}_{ab}$ , was parallel to the twin boundaries ( $\mathbf{I}_{ab} \parallel \text{TB}$ ), as it is schematically shown in the corresponding insets of Fig. 2. Electric contacts were created using the standard four-probe arrangement by depositing silver paste onto the crystal surface and affixing silver wires followed by 3 h annealing at 200°C in oxygen atmosphere. The conductors for the current contacts were made of foil with 0.1 mm thickness and a width of 2 mm and for potential contacts we used wire diameter of 0.05 mm. Such production procedure allowed us to obtain the contacts with small transfer resistance permitting to measure the resistance at transport currents up to 1 A without overheating the contacts. Electrical resistivity and current-voltage characteristics measurements were carried out at constant current. The magnetic field of 12.7 kOe was created by an electromagnet. The magnet rotation allowed varying the orientation of the field relative to the crystal. The accuracy of field orientation relative to the sample was better than 0.2°. Bridge was mounted in the measuring cell in a position that the field vector  $\mathbf{H}$  was always perpendicular to the transport current

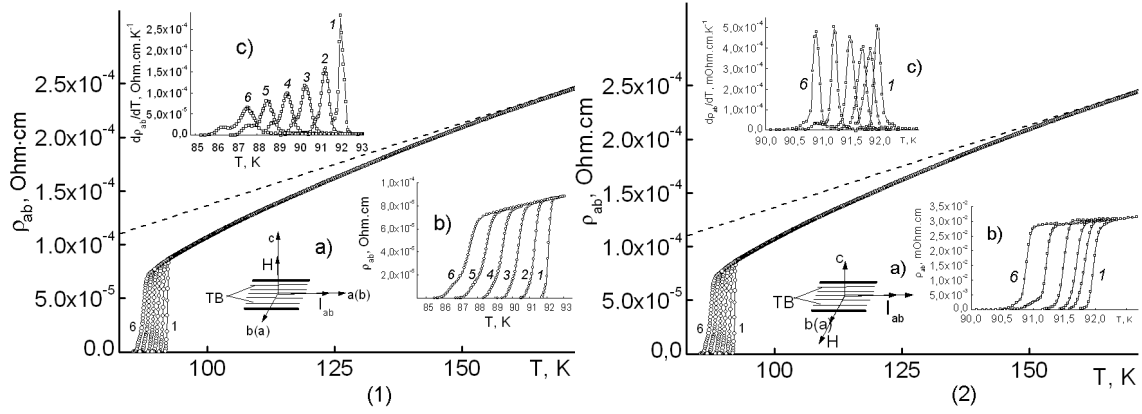


Fig. 2. Temperature dependence of the resistivity  $\rho_{ab}(T)$  of  $\text{YBa}_2\text{Cu}_{3-z}\text{Al}_2\text{O}_{7-\delta}$  single crystal in the orientation of the field vector  $\mathbf{H} \parallel \mathbf{c}$  (1) and  $\mathbf{H} \perp \mathbf{c}$  (2) for  $H$ , kOe: 0, 1.9, 4.5, 7.3, 10, 12.7 — curves 1–6, respectively. The dotted line shows extrapolation of the linear area of the experimental curve. The insert (a) shows a schematic representation of the geometry of the experiment. Insert (b) and (c) — transitions into the superconducting state in the coordinates  $\rho_{ab} - T$  and  $d\rho_{ab}/dT - T - T$ , respectively. The numbering of the curves in the insets corresponds to the numbering in Fig.

vector. Temperature measurement accuracy was 0.005 K. Temperature stability during the measurements was better than 0.01 K.

### 3. Results and discussion

The comparative analysis of the resistive characteristics of  $\text{YBa}_2\text{Cu}_3\text{O}_{7-\delta}$  and  $\text{YBa}_2\text{Cu}_{3-z}\text{Al}_2\text{O}_{7-\delta}$  single crystals in zero magnetic field has been performed in the previous works [2, 3]. Temperature dependences of the resistivity in  $ab$ -plane  $\rho_{ab}(T)$  in magnetic fields up to 12.7 kOe for the orientations of the field vector  $\mathbf{H} \parallel \mathbf{c}$  and  $\mathbf{H} \perp \mathbf{c}$  are shown in Fig. 2 (1) and (2), respectively. The resistive transitions to the superconducting state of the same samples in coordinates  $\lg \rho_{ab} - T$  and  $d\rho_{ab}/dT - T$  are shown in the relevant insets.

The critical temperature of the crystal at zero magnetic field, which is determined by the maximum on  $d\rho_{ab}(T)/dT$  at a region of resistive transition to the superconducting state [2], was equal to 92.1 K with a transition width  $\Delta T_c \leq 0.5$  K. The electrical resistivity in  $ab$ -plane at room temperature was about 420  $\mu\text{Ohm-cm}$ . According to the literature, the high values of the critical temperature  $T_c \approx 92$  K correspond to the aluminum concentration in the crystal  $z \leq 0.05$  [10], and the oxygen content of  $\delta \leq 0.1$  [11]. At the same time, the narrow width of the superconducting transition  $\Delta T_c \leq 0.5$  K indicates a uniform distribution of oxygen and Al in the crystal.

As can be seen from Fig. 2, under the temperature lowering from 300 K to 200 K

the  $\rho_{ab}$  decreases practically linearly that indicates quasimetallic conductivity behavior in this temperature range. The magnetic field, in both orientations, has almost no effect on the behavior of dependences  $\rho_{ab}(T)$  at  $T \geq 1.1 T_c$ , that is consistent with the published data for samples of  $\text{YBaCuO}$ , obtained from magnetoresistance measurements [12]. An influence of the magnetic field reveals mainly by a shift down the resistive transition temperature to the superconducting state and a corresponding reduction of  $T_c$  (insets (b) and (c)), as more detail will be described below. At the same time, at temperatures  $T_c < T < 200$  K a deviation of  $\rho_{ab}(T)$  from linearity indicates an appearance of the excess conductivity, the temperature dependence of which is usually determined as follows from the experimental data, such as:

$$\Delta\sigma = \sigma - \sigma_0, \quad (1)$$

where  $\sigma_0 = \rho_0^{-1} = (A + BT)^{-1}$  is the conductivity, determined by extrapolating the linear segment backward to zero temperature and  $\sigma = \rho^{-1}$  is experimentally determined value of conductivity in the normal state.

It is known from previous theoretical work [13], that near  $T_c$  the  $\Delta\sigma$  is conditioned by the processes of the carriers fluctuation pairing and in general terms, depending from the dimension of the system is determined by the following equation:

$$\Delta\sigma_D = A_D \varepsilon^{-\alpha}, \quad (2)$$

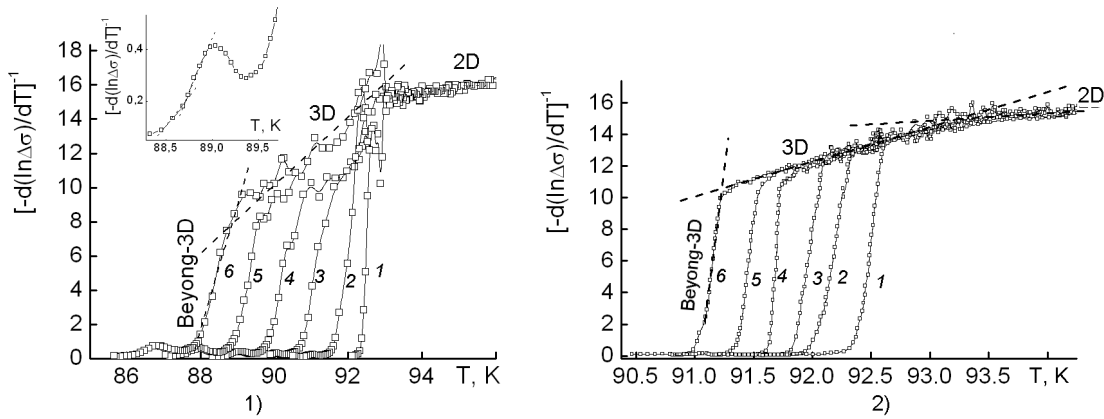


Fig. 3. Resistive transitions into the superconducting state of an  $\text{YBa}_2\text{Cu}_3\text{Al}_2\text{O}_{7-5}$  single crystal for  $H$ , kOe: 0 (1), 1.9 (2), 4.5 (3), 7.3 (4), 10 (5), 12.7 (6). Insert: low-temperature section of a resistive transition, measured in field  $H = 7.3$  kOe. The dashed lines in the figure and insert show the extrapolation of the sections corresponding to different FC regimes.

where  $A_d$  is a constant and  $\varepsilon = (T - T_c)/T_c$  is the reduced temperature. Herewith, the exponent  $\alpha$ , is defined, according to [13–15], as  $\alpha = 2 - D/2$ , where  $D$  is a dimension of the system. In particular, at  $T > T_c$  for two-dimensional (2D) and three-dimensional (3D) cases, the temperature dependence of  $\Delta\sigma$  is determined by power relations of the form [13]:

$$\Delta\sigma_{2D} = A_{2D}\varepsilon^{-1}, \quad (3)$$

$$\Delta\sigma_{3D} = A_{3D}\varepsilon^{-1/2}, \quad (4)$$

where  $A_{2D} = e^2/16\hbar d$  and  $A_{3D} = e^2/32\hbar\xi_c(0)$ ;  $\xi_c$  is the coherence length along the  $c$  axis for  $T \rightarrow 0$  and  $d$  is a characteristic size of the two-dimensional layer.

Thus, once  $[-d(\ln(\Delta\sigma)/dT)]^{-1} = \alpha^{-1}(-T_c)$  has been calculated from the experimental data the method proposed in [14] and elaborated in [15], can be used to determine a dimensionality of the subsystem and a character of the fluctuation-carrier scattering [13] in different temperature intervals from the slope angle of the curves in the appropriate coordinates. Fig. 3 shows the resistive transitions of  $\text{YBa}_2\text{Cu}_3\text{O}_{7-\delta}$  single crystal in the coordinates  $[-d(\ln\Delta\sigma)/dT]^{-1} - T$  obtained for different values of the magnetic field.

As once can be seen in Fig. 3, in both orientations of the magnetic field, the experimental curves in the immediate proximity of  $T_c$  are characterized by the presence of two distinct sections with different slope angles, which, apparently, correspond to the

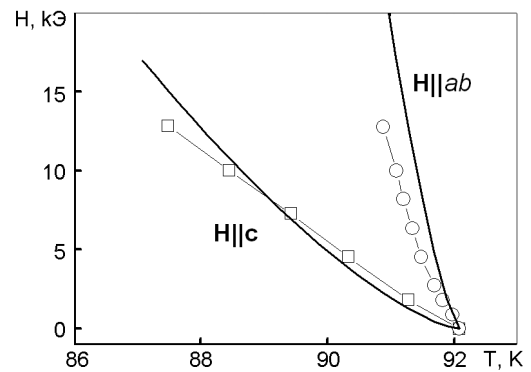


Fig. 4. Temperature dependences of the second critical field for its parallel and perpendicular orientation relative to the basal plane. Solid lines – calculation for the same geometry of the experiment, carried out according to [16].

so-called beyond-3D and 3D regimes [15] with  $\alpha \approx 0.17$  and  $0.5$ , respectively. As temperature increases away from  $T_c$ , the absolute value of  $a$  increases, which could indicate an occurrence of the 3D–2D crossover transition in the system; more details about this will be given below.

The second feature of the obtained dependence is that we observe the equidistant shift of the resistive transition to the superconductive (SC) state downwards in temperature with increasing of the applied magnetic field. In this case, when the experimental geometry  $\mathbf{H}||c$  there was a slight broadening of the experimental curves, while in the case of  $\mathbf{H}||c$  expansion was not observed at all.

As it was noted above, this effect is observed only in the case of aluminium-doped samples [1] in contrast to all other 1-2-3 compounds, for which, the clearly expressed

"fan-shaped" expansion of the SC transition in the magnetic field is a characteristic feature [4–7]. Fig. 4 shows the  $H-T_c$  dependence, obtained for our experimental curves and determined by the maximum of derivative  $d\rho/dT(T)$  in the area of the SC transition [2].  $T_c$  monotonically decreases with an increase of the magnetic field. The strongly nonlinear current voltage characteristics up to a certain line of  $T_M(H)$ , is the characteristic feature of the 1-2-3 compounds and corresponds to the transition from the no pinning vortex liquid state (experiencing viscous flow under the action of Lorentz force) to the state pinning vortex glass state [16]. According to [16] the line of this transition in magnetic field  $\mathbf{H}\parallel\mathbf{c}$  and  $\mathbf{H}\perp\mathbf{c}$  in the case of untwinned samples is determined by the expressions  $H_M^{\parallel}(T) = 103(1-T/T_c)^{1.41}$  and  $H_M^{\perp}(T) = 842(1-T/T_c)^{1.37}$ , respectively. As can be seen from Fig. 4 in our case, these lines (solid line) are located partially ( $\mathbf{H}\parallel\mathbf{c}$ ) or full ( $\mathbf{H}\perp\mathbf{c}$ ) above, our experimental curves, which may indicate the absence of the non pinning vortex liquid phase in the samples. This, in its turn, may cause the lack of a corresponding expansion of the resistive transitions in the magnetic field. The existence of a developed TB system in our samples can be important as they are very strong pinning centres. The latter supposition is supported by the third important feature of the experimental curves: the presence of a small additional peak in the curves  $[-d(\ln Aa/dT)]^{-1}-T$  for  $\mathbf{H}\parallel\mathbf{c}$ , which is absent in zero magnetic field and manifests most strongly in strong magnetic fields. An enlarged section of the curve with such a maximum, obtained in magnetic field 12 kOe, is shown in the inset in Fig. 3. It is evident that at temperatures below the peak our dependence is characterized by the slope angles  $a = 1.27$  and  $2.2$ . According to theory [17] the latter value corresponds to a paracoherent transition at the intergrain and interdomain boundaries, which is often observed in different classes of superconducting compounds [15, 17]. In our case TBs can play the role of such boundaries.

Therefore, impurities can play a critical role. As we know from the literature [18, 19] the trivalent impurities are defect centers and for the increased concentration of defects the period of the domain twin structure decreases. As a result, a close overlap of micro-twins and the formation of tweed structure is taking place [18, 19]. As shown by metallographic investigations [19], in the crystals  $\text{YBa}_2\text{Cu}_3\text{O}_{7-\delta}$  the "tweed" structure

is not observed, which is probably due to the low concentration of Al. Meanwhile the inter-boundary distance was two or three times smaller than in pure crystals. Obviously, in our case, the cause of reducing the period of the domain structure could be the influence of impurity atoms of aluminum, having a much smaller ionic radius comparing with copper. Besides this, aluminum atomic position (000) may form a characteristic octahedral environment for oxygen atoms.

It should be noted that at  $\mathbf{H}\perp\mathbf{c}$  geometry of the experiment the similar characteristics in the form of additional peak, almost did not reveal in the weak magnetic fields, and were much less expressed in the region of maximum magnetic field (Fig. 3). Such differences, apparently, can be the result of a specific mechanism for the pinning of superconducting fluctuations. Thus, in the case of  $\mathbf{H}\perp\mathbf{c}$  the Lorentz force acting on the fluctuating carriers  $\mathbf{F}_L - [\mathbf{j} \times \mathbf{H}]$  is directed along the twin boundaries ( $\mathbf{F}_L \parallel \text{TB}$ ), and in the case of  $\mathbf{H}\parallel\mathbf{c}$ , respectively, across ( $\mathbf{F}_L \perp \text{TB}$ ), which in turn causes several times more enhanced pinning force of superconducting fluctuations in the second case compared to the first. The last assumption is confirmed by non-monotonic behavior of the field dependence  $\xi_c(H)$  observed in the case of  $\mathbf{H}\parallel\mathbf{c}$ .

As shown in [20], the fluctuation conductivity  $\Delta\sigma(T, H)$  of layered superconductors in a magnetic field can be written in the general form:

$$\Delta\sigma(T, H) = \Delta\sigma_{AL}(T, H) + \Delta\sigma_{MT}(T, H), \quad (5)$$

where

$$\begin{aligned} \Delta\sigma_{AL}(T, H) &= \quad (6) \\ &= \frac{e^2}{16\hbar d\epsilon} \left\{ \frac{1}{(1+2\alpha)^{1/2}} - \frac{(2+4\alpha+3\alpha^2)b^2}{4(1+2\alpha)^{5/2}\epsilon^2} + \dots \right\} \end{aligned}$$

is Aslamazov-Larkin fluctuation conductivity [13];

$$\begin{aligned} \Delta\sigma_{MT}(T, H) &= \quad (7) \\ &= \frac{e^2}{8\hbar d(1-\alpha/\delta)\epsilon} \left\{ \ln \left( \frac{\delta(1+\alpha+\sqrt{1+2\alpha})}{\alpha(1+\delta+\sqrt{1+2\delta})} \right) - \left[ \frac{\delta^2}{\alpha^2} \frac{1+\delta}{1+2\delta)^{3/2}} - \frac{1+\alpha}{1+2\alpha)^{3/2}} \right] \frac{b^2}{6\epsilon} + \dots \right\} \end{aligned}$$

is Maki-Thompson fluctuation conductivity, which is due to interaction of the unpaired carriers with the fluctuation Cooper pairs [21];  $\alpha = 2\xi_c^2(0)/d^2\epsilon$ ;  $b = (2e\xi_{ab}^2(0)/\hbar H$ ;  $\delta = (16/\pi)(\xi_c^2(0)/d^2) (kT\tau_\phi/\hbar h)$ ;  $\xi_{ab}(0)$  is the

coherence length in the basal plane, and  $\tau_\phi$  is the characteristic order-parameter interference time. Other designations are the same as in (3) and (4).

Setting  $\xi_c(0) \approx 2.5 \text{ \AA}$ ,  $d \approx 11.7 \text{ \AA}$  [22],  $\tau_\phi \approx \hbar/2k_B T_c$ , the evolution of the relative contribution of each component in (5)  $\Delta\sigma_{AL}/\Delta\sigma_{MT}$  as the temperature increases away from the superconducting transition point in zero magnetic field can be evaluated as proposed in [23]. Analysis of expressions (6) and (7) shows that although in the temperature interval  $T_c < T < 1.25T_c$  the component  $\Delta\sigma_{MT}(T, H = 0)$  shows a much weaker temperature dependence than  $\Delta\sigma_{AL}(T, H = 0)$ , the ratios  $\Delta\sigma_{AL}/\Delta\sigma_{MT}$  decrease by more than a factor of two (about 4 to 1.7) as temperature increases from  $1.005T_c$  and  $1.25T_c$ . In turn, this could attest to a substantial growth of the intensity of fluctuation pair scattering.

It should be also noted that, according to the analysis, all the dependencies of  $\Delta\sigma(T, H)$  in the range of  $1.1 - 1.15T_c$  satisfactorily approximated by the dependence of the form (3) corresponding to the two-dimensional case (see the inset in Fig. 5), while for  $T < 1.05 T_c$  the behavior of  $\Delta\sigma(T, H)$  (inset in Fig. 5) corresponds well to the dependence (4) for the three-dimensional case. In this case, having determined  $\varepsilon_0$  at the point 2D–3D crossover at intersection of two straight lines corresponding to the exponents  $-0.5$  and  $-1$  in the dependences  $\ln\Delta\sigma - \ln\varepsilon$ , and using the published data on the dependence of the interplanar distance from  $\delta$  [22] ( $d = 11.7 \text{ \AA}$ ), the value of  $\xi_c(0)$  can be determined.

From Fig. 5, which shows the field dependences  $\xi_c(0, H)$  for two orientations of the magnetic field, it is clear that the orientation of  $\mathbf{H} \perp \mathbf{c}$  a curve  $\xi_c(0, H)$  is characterized by a distinct peak near magnetic fields  $H = 2 \text{ kOe}$ . At the same time, at orientation  $\mathbf{H} \parallel \mathbf{c}$  the curve gradually decreases with increasing the magnetic field. It should be noted that this feature which manifested in the form of a non-monotonic dependence of the critical current  $j_c$  from the magnetic field (peak effect), is often observed in HTSC — systems with parallel orientation of the magnetic field as a consequence of the specific mechanism of vortex pinning matter [24, 25]. The curve with circles in Fig. 5 shows the field dependence of  $j_c(H)$  with the magnetic field  $\mathbf{H} \parallel \mathbf{c}$  which we obtained by determining the critical current

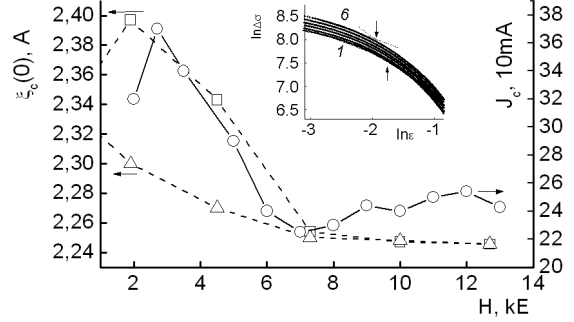


Fig. 5. Field dependences  $\rho_c(0, H)$  in the orientation of the field vector  $\mathbf{H} \parallel \mathbf{c}$  and  $\mathbf{H} \perp \mathbf{c}$  (squares and triangles, respectively) and the critical current for the magnetic field orientation  $\mathbf{H} \parallel \mathbf{c}$  (circles). Insert shows the temperature dependences of the excess conductivity in  $ab$ -plane coordinates  $\ln\Delta\sigma - \ln\varepsilon$  for different values of the magnetic field for orientation  $\mathbf{H} \parallel \mathbf{c}$ . Designation of the curves in the insert corresponds to the notation in Fig. 2. The dotted lines in the insert shows the approximation of the experimental curves with a straight angle  $\text{tg}\alpha_1 \approx -0.5$  (3D — regime) and  $\text{tg}\alpha_1 \approx -1.0$  (2D — regime). The arrows indicate the point of 2D–3D crossover.

in terms of voltage drop on the current-voltage characteristics of the technique [6, 7]. In this case, it is clear that the position of the characteristic maximum in the dependences  $j_c(H)$  correlates well with the case with  $\xi_c(0, H)$ . According to [25], one of the possible reasons for the appearance of the peak effect may be the presence in the sample is deficient in oxygen or another phase, turning into a normal state with increasing the magnetic field. In this case, the role of this phase can play TB, which (as defects higher dimension) can be effective centers for vacancy sink [9, 26, 27], and, accordingly, have lower (compared to the rest of the sample) oxygen content. The assumption of the presence of a phase with lower  $T_c$ , confirmed the presence of step-wise resistive transitions and a small additional maximum on  $d\rho_{ab}(T)/dT$  (inset (b) and (c) to Fig. 2) observed in the orientation of  $\mathbf{H} \parallel \mathbf{c}$  that becomes most expressed at the maximum values of the magnetic field. Thus experiments of decorating the vortex structure [27] really show that the density of vortices on TB increased compared to their density in the bulk superconductor, indicating about suppression of order parameter on TB. In our case this feature is probably due to some suppression of the excess fluctuation conductivity with increasing dissipation, because of the displacement

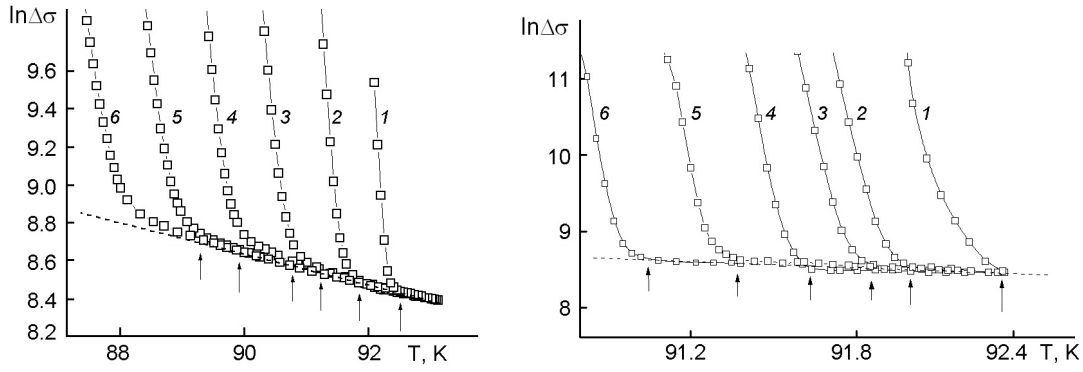


Fig. 6. Temperature dependences of the excess conductivity for the magnetic field orientation  $\mathbf{H}\parallel\mathbf{c}$  and  $\mathbf{H}\perp\mathbf{c}$  in the coordinate's  $\ln\Delta\sigma - T$ . The numbering of the curves corresponds to the numbering in Fig. 2.

of the superconducting fluctuations in the sample by Lorentz force. In turn, a decrease of  $\Delta\sigma$ , according to (4), should result in an increase of  $\xi_c(0,H)$ , that is in fact observed in our case. At the following field increasing, its effect will be expressed by decrease of the fluctuations correlation function, which should be expressed in a decrease of the pinning force of the fluctuations [25] and in an increase of the gradient of the characteristic volume density of the fluctuation energy. Certain role it can play in the effort to strengthen of the some specific mechanisms of the quasi-particle interaction [28, 29]. In this case  $\xi_c(0,H)$  will decrease instead of increase.

It should also be noted that if the FC transition temperature,  $T_f$ , is determined according to the point where  $\ln\Delta\sigma$  shifts upwards from the linear dependence  $\ln\Delta\sigma(T)$  [3] (see Fig. 6), then the relative width of the region of existence of the FC regime can be estimated as  $t_f = (T_f - T_c)/T_c$ . The computational results show that a magnetic field causes a general relative narrowing of the temperature interval of an occurrence of fluctuation paraconductivity. It should be noted that the orientation of the magnetic field  $\mathbf{H}\parallel\mathbf{c}$  a relatively small constriction (from  $t_f \approx 0.1594$  in zero magnetic field to  $t_f \approx 0.1473$  at  $H = 12.7$  kOe), whereas when the magnetic field  $\mathbf{H}\perp\mathbf{c}$  narrowing occurs almost twice (from  $t_f \approx 0.0214$  in zero magnetic field to  $t_f \approx 0.0417$  at  $H = 12.7$  kOe). This is probably due to the suppression of long-wavelength fluctuations with increasing the magnetic field, which make the largest contribution to the paraconductivity near  $T_c$ . At the same time, as shown in [2], underestimation of the contribution of the short-wavelength fluctuations of the order parameter results in a more rapid than

theoretically predicted decrease of  $\Delta\sigma$  at temperatures sufficiently above  $T_c$ . Microscopic calculation of the fluctuation correction of the conductivity with taking account of all components of the order parameter has been performed in [30]. Comparison of our data with their theory [30] showed that  $\Delta\sigma$  (in our experimental error) can be described on the basis of the FC theory at temperatures close to  $1.25T_c$ . This is probably the temperature range where transition to the pseudogap regime occurs; we have analyzed this transition in detail in [2, 3, 31–35].

#### 4. Conclusions

In summary, it can be concluded from the mentioned above that twinning boundaries in  $\text{YBa}_2\text{Cu}_{3-2z}\text{Al}_2\text{O}_{7-5}$  ( $z \leq 0.5$ ) single crystals are effective fluctuation-carrier scattering centers. The deviation from linearity of the temperature dependences  $\rho_{ab}(T)$  for  $T_c < T < 1.35T_c$  can be satisfactorily explained on the basis of the theory of fluctuation superconductivity. The three-dimensional Aslamazov-Larkin model describes well FC close to  $T_c$ . Application of a magnetic field causes strong narrowing of the temperature interval of the existence of three-dimensional fluctuations. The non-monotonic dependence of  $\xi_c(0)$  on the magnetic field is probably due to the suppression of the excess fluctuation conductivity in the weak magnetic fields. The lack of fan-shaped expansion of the resistive transitions in the magnetic field (characteristic for the undoped samples  $\text{Y}_1\text{Ba}_2\text{Cu}_3\text{O}_{7-\delta}$ ) in these samples may be due to the lack of the no pinning vortex liquid phase due to increased pinning of the vortex lattice at the twin boundaries.

This work was supported in part by European Commission CORDIS Seven Framework Program, Project No.247556.

### References

1. R.H.Koch, V.Foglietti, W.J.Gallagher, *Phys. Rev. Lett.*, **68**, 1511 (1989).
2. R.V.Vovk, M.A.Obolenskii, A.A.Zavgorodniy, A.V.Bondarenko et al., *J.Mater. Sci.:Mater. Electron.*, **18**, 811 (2007).
3. R.V.Vovk, M.A.Obolenskii, A.A.Zavgorodniy et al., *Physica B*, **404**, 3516 (2009).
4. R.V.Vovk, Z.F.Nazyrov, M.A.Obolenskii et al., *Journal of Alloys and Compounds*, **509**, 4553 (2011).
5. N.Ya. Fogel, I.M. dmitrenko, V.G. Cherkasova, *SFKaT*, **2**, 115 (1989)
6. A.V.Bondarenko, V.A.Shklovskij, M.A.Obolenskii et al., *Phys. Rev. B*, **58**, 2445 (1998).
7. A.V.Bondarenko, A.A.Prodan, M.A. Obolenskii et al., *Low Temp.Phys.*, **27**, 339,(2001) [*Fizika Nizkikh. Temp*], **27**,463, (2001).
8. T.K.Worthington, F.H.Holtzberg, C.A.Field, *Cryogenics*, **30**, 417 (1990).
9. R.V.Vovk, Z.F.Nazyrov, M.A.Obolenskii et al., *Philosophical Magazine*, **91**, 2291 (2011).
10. R.B.Van Dover, L.F.Schneemeyer, J.V.Waszczak et al., *Phys. Rev. B*, **39**, 2932 (1989).
11. R.V.Vovk, M.A.Obolenskii, A.V.Bondarenko et al., *J.Alloys and Compaunds*, **464**, 58 (2008).
12. R.V.Vovk, V.M.Gvozdikov, M.A.Obolenskii et al., *Acta Physica Polonica A*, **121**, 1191 (2012).
13. L.G.Aslamazov, A.L.Larkin, *Sov. Phys. Solid State*, **10**, 3258 (1968)
14. J.S.Kouvel, M.E.Fischer, *Phys. Rev.*, **136**, A1616 (1964).
15. R.M.Costa, I.C.Riegel, A.R.Jurelo, J.L.Pimentel Jr., *Journal of Magnetism and Magnetic Materials*, **320**, e493 (2008).
16. W.K.Kwok et al., *Phys. Rev. Lett.*, **69**, 3370 (1992).
17. J.Rosenblatt, in: Percolation, Localization and Superconductivity, NATO ASI Series, ed. by A.M.Goldman and S.A.Wolf, Plenum, New York (1984), p.431.
18. G.Lacaye, R.Hermann, G.Kaestener, *Physica C*, **192**, 207 (1992).
19. R.V.Vovk, M.A.Obolenskii, Z.F.Nazyrov et al., *J. Mater. Sci.:Mater. Electron.*, **23**, 1255 (2012).
20. S.Hikami, A.I.Larkin, *Modern Phys. Lett.*, **B2**, 693 (1988).
21. J.B.Bieri, K.Maki, R.S.Thompson, *Phys. Rev. B*, **44**, 4709 (1991).
22. G.D.Chryssikos, E.I.Kamitsos, J.A.Kapoutsis et al., *Physica C*, **254**, 44 (1995).
23. N.E. Alekseevskii, A.V.Mitin, V.I. Nizhankovskii, et al., *Sverkhprovodimost' Fiz., Khim, Tekhn.*, **2**, 40 (1989).
24. D.A.Lotnyk, R.V.Vovk, M.A.Obolenskii et al., *Journal of Low Temperature Physics*, **161**, 387 (2010).
25. M.Daeumling, J.M.Seutjens, D.C.Larbalestier, *Nature. London*, **346**, 332 (1990).
26. G.Blatter, M.V.Feigel'man, V.B.Geshkenbein et al., *Rev. Mod. Phys.*, **66**, 1125 (1994).
27. L.Y.Vinnikov, L.A.Gurevich, G.A.Yemelchenko, Y.A.Ossipyan, *Solid State Commun.*, **67**, 421 (1988).
28. D.H.S.Smith, R.V.Vovk, C.D.H.Williams, A.F.G.Wyatt, *Phys. Rev. B*, **72**, 0546506 (2005).
29. D.H.S.Smith, R.V.Vovk, C.D.H.Williams, A.F.G.Wyatt, *New Journal of Physics*, **8**, 128 (2006).
30. L.Reggani, R.Vaglio, A.A.Varlamov, *Phys. Rev. B*, **44**, 9541 (1991).
31. R.V.Vovk, A.A.Zavgorodniy, M.A.Obolenskii et al., *Modern Physics Letters B (MPLB) Condensed Matter Physics; Statistical Physics and Applied Physics*, **24**, 2295 (2010).
32. R.V.Vovk, M.A.Obolenskii, A.A.Zavgorodniy et al., *J. Mater. Sci.: Mater. in Electron.*, **20**, 858 (2009).
33. R.V.Vovk, M.A.Obolenskii, A.A.Zavgorodniy et al., *J. Alloys Compd.*, **485**, 121 (2009).
34. R.V.Vovk, A.A.Zavgorodniy, M.A.Obolenskii et al., *Journal of Materials Science: Materials in Electronics*, **22**, 20 (2011).
35. R.V.Vovk, Z.F.Nazyrov, I.L.Goulatis, A.Chroneos, *Modern Physics Letters B (MPLB) Condensed Matter Physics; Statistical Physics and Applied Physics*, **26**, 1250163 (2012).



**Вплив поперечного та поздовжнього магнітного поля  
на надлишкову провідність монокристалів  
 $\text{YBa}_2\text{Cu}_{3-z}\text{Al}_z\text{O}_{7-\delta}$  з заданою топологією  
плоских дефектів**

***Р.В.Вовк, З.Ф.Назирова, Г.Я.Хаджай,  
V.M.Pinto Simoes, V.V.Kruglyak***

Досліджено вплив постійного магнітного поля до 12,7 кЕ на температурні залежності електропровідності у базовій *ab*-площині легованих алюмінієм монокристалів  $\text{YBaCuO}$  з системою односпрямованих двійникових меж. Встановлено, що двійникові межі є ефективними центрами розсіювання флуктуаційних носіїв. Безпосередньо поблизу  $T_c$  температурні залежності надлишкової паропровідності задовільно описуються у рамках теоретичної моделі флуктуаційної провідності Хікамі-Ларкіна для шаруватих надпровідних систем. Обговорюються причини пригнічення тривимірних надпровідних флуктуацій та немонотонної залежності  $\xi_c(0, H)$  у слабких магнітних полях при орієнтації вектора магнітного поля вздовж осі *c*. Показано, що відсутність "віялоподібного" розширення резистивних переходів у магнітному полі, характерного для бездомішкових зразків  $\text{YBa}_2\text{Cu}_{3-z}\text{Al}_z\text{O}_{7-\delta}$ , обумовлено пригніченням фазового переходу до стану незапінігваної вихорової рідини внаслідок посилення піннінгу вихрової решітки на двійникових межах.